

Inal Chem. Author manuscript; available in PMC 2008 September 22.

Published in final edited form as:

Anal Chem. 2007 April 1; 79(7): 2688–2694. doi:10.1021/ac061597p.

Design and Characterization of a High-power Laser-induced Acoustic Desorption (LIAD) Probe Coupled with a Fouriertransform Ion Cyclotron Resonance Mass Spectrometer

Ryan C. Shea[†], Steven C. Habicht, Weldon E. Vaughn, and Hilkka I. Kenttämaa^{*}
Department of Chemistry, Purdue University, 560 Oval Drive, West Lafayette, IN 47907-2084

Abstract

We report here the construction and characterization of a high-power laser-induced acoustic desorption (LIAD) probe designed for Fourier-transform ion cyclotron resonance (FT-ICR) mass spectrometers to facilitate analysis of non-volatile, thermally labile compounds. This "next generation" LIAD probe offers significant improvements in sensitivity and desorption efficiency for analytes with larger molecular weights via the use of higher laser irradiances. Unlike the previous probes which utilized a power limiting optical fiber to transmit the laser pulses through the probe, this probe employs a set of mirrors and a focusing lens. At the end of the probe, the energy from the laser pulses propagates through a thin metal foil as an acoustic wave, resulting in desorption of neutral molecules from the opposite side of the foil. Following desorption, the molecules can be ionized by electron impact or chemical ionization. Almost an order of magnitude greater power density (up to 5.0×10^9 W/cm²) is achievable on the backside of the foil with the high-power LIAD probe compared to the earlier LIAD probes (maximum power density $\sim 9.0 \times 10^8$ W/cm²). The use of higher laser irradiances is demonstrated not to cause fragmentation of the analyte. The use of higher laser irradiances increases sensitivity since it results in the evaporation of a greater number of molecules per laser pulse. Measurement of the average velocities of LIAD evaporated molecules demonstrates that higher laser irradiances do not correlate with higher velocities of the gaseous analyte molecules.

Introduction

In recent years, laser-induced acoustic desorption $^{1-3}$ (LIAD) coupled with Fourier transform ion cyclotron resonance mass spectrometers 4 (FT-ICR) has been demonstrated to provide a useful analysis method for a wide variety of nonvolatile, thermally labile compounds, including those that previously could not be analyzed by mass spectrometry. $^{4-9}$ The LIAD technique utilizes laser generated shockwaves to desorb neutral analyte molecules into a mass spectrometer. A thin layer of the analyte is deposited onto a thin (12.7 μ m) Ti foil and the opposite side (backside) is irradiated by a series of short (3 ns) high intensity (~ 2.5 mJ/pulse) laser pulses (532 nm). The laser energy is propagated through the foil as an acoustic wave, resulting in desorption of low-energy neutral analyte molecules from the opposite side of the foil into the mass spectrometer. Several LIAD characterization studies have been carried out, including investigation of the influence of several experimental variables have been carried out, including investigation of the LIAD evaporated molecules. In Ionization of the desorbed molecules by well characterized chemical reactions has been demonstrated to be an effective approach for the analysis of non-volatile, thermally labile compounds. 5,6

^{*}To whom correspondence should be addressed. Email: hilkka@purdue.edu.

[†]Current address: BP Chemicals, Aromatics & Acetyls, Naperville, IL 60563

One of the limitations of LIAD experiments, as utilized in our laboratories, is the inability to analyze species with large molecular weights. Depending on the type of analyte being studied, different high mass limits exist. For example, the analysis of peptides is limited to molecules of less than approximately 500 amu, while a much higher limit of approximately 1200 amu applies for saturated hydrocarbon polymers. These limits are believed to be related to the amplitude of the acoustic wave generated within the metal foil $^{12-14}$ and the different strengths of analyte/surface interactions.

One of the studies that have been performed to characterize LIAD included evaluating the signal intensities and distribution of polyisobutenyl succinic anhydride (PIBSA) oligomers detected after LIAD/CI (deprotonation with bromide ion) as a function of laser power density (irradiance, W/cm²) on the backside of the foil. 15 The results indicate that higher irradiances aid in the evaporation of molecules of higher molecular weights, likely because larger amplitude acoustic waves are generated. 16 These trends were observed for power densities ranging from 5.4×10^8 W/cm² to 9.0×10^8 W/cm² and are attributed to the generation of acoustic waves with larger amplitudes within the Ti foil.

The above results prompted us to employ the use of greater laser irradiances to improve the desorption efficiency of species with larger molecular weights. Thus far, the LIAD experiments have been performed through the use of two specially designed LIAD probes 4,10,17 which utilize an optical fiber to transmit the laser pulses the length of the probe to the sample foil. The power density achievable on the backside of the foil with these probes is limited due to the damage threshold ($^{4.5}$ mJ/pulse) of the optical fiber.

A variety of approaches could be employed to increase the power density on the backside of the foil, including tighter focusing, reducing the laser pulse width (requiring the use of a different laser), and utilizing greater input laser powers. In order to overcome this limitation, a LIAD probe was designed that does not use a power limiting optical fiber and hence allows the use of a greater amount of the available input laser power. This high-power laser probe utilizes a series of mirrors and lenses to reflect and focus the high intensity laser pulses (up to ~ 25 mJ/pulse maximum laser output) onto the backside of the Ti foil. This probe allows almost an order of magnitude greater power density (up to 5.0×10^9 W/cm²) on the backside of the sample foil which aids in the evaporation of molecules with larger molecular weights.

Experimental

Two Fourier-transform ion cyclotron resonance mass spectrometers, (FT-ICR) of similar configuration were used for the experiments described here. The experiments were performed using either a Nicolet model FTMS 2000 dual cell FT-ICR or an Extrel model FTMS 2001 dual cell FT-ICR. Each instrument was equipped with a 3 T superconducting magnet and a differentially pumped dual cell, as described previously. 6,18 The Nicolet FT-ICR utilized two Edwards Diffstak 160 diffusion pumps (700 L/s), each backed by an Alcatel 2010 (3.2 L/s) dual rotary-vane pump, for differential pumping. The Extrel FT-ICR utilized two Balzer TPU turbomolecular pumps (330 L/s) (each backed by an Alcatel 2010 (3.2 L/s) dual rotary-vane pump) instead of diffusion pumps. The nominal baseline pressure in both instruments is $<10^{-9}$ torr inside the vacuum chamber, as measured by Bayard-Alpert ionization gauges located on each side of the dual cell. In each instrument, the cells are separated by a common wall (the conductance limit) which contains a 2 mm hole in the center. Unless otherwise noted, this plate and the other two trapping plates were maintained at +2 V.

Both instruments (Figure 1) are equipped with a commercial manual insertion probe inlet, which is also used for the LIAD probes (fiber and fiberless). Details of the optical fiber containing LIAD (7/8" outer diameter) probe have been described previously. ^{10,17} Both LIAD probes (fiber and fiberless) employed a Nd:YAG laser (Minilite II, Continuum Lasers; 532

nm, 25 mJ/pulse (max), 3 ns pulse width) whose beam was focused onto the backside of a sample metal foil over an irradiation area of approximately 10^{-3} cm².

Fiberless LIAD was accomplished with the use of a novel probe which utilizes a series of reflecting mirrors and lenses to direct the laser beam down the length of the probe and onto the backside of the metal foil. The laser beam reflection and focusing region of the fiberless LIAD probe (the Nicolet instrument) is detailed in Figure 2. The fiberless LIAD probe consists of a hollow stainless steel outer cylinder (0.875 in o.d., 0.767 in i.d.) with a removable threaded sample holder that contains an epoxy vacuum sealed transparent window (Almaz Optics, Fused Silica, 17.5 mm diameter × 3.0 mm thickness). The threaded sample holder is screwed into the threaded end of the outer cylinder and further sealed with a pair of Viton fluoroelastomer orings (Applied Industrial Technologies). An o-ring of 18 mm o.d. and one of 19 mm o.d. (both of 1 mm thickness) were used to seal the sample holder with the outer cylinder. The sealed window maintains vacuum integrity between the high vacuum region ($<10^{-9}$ torr) and the atmospheric region inside the probe when inserted into the mass spectrometer. With a set of Teflon rings, the sample holder is designed to maintain the sample foil and glass cover slip (Fisher Scientific, $200 \, \mu \text{m}$ thickness) at a fixed distance from the window. Similar to the design of a previous LIAD probe, ^{10,17} the outer cylinder of the fiberless LIAD probe, to which the sample foil is secured, can be rotated within the magnetic field to achieve additional sampling spots on the foil. The desorption axis is held stationary and is in alignment with the center of the ICR cell. With similar dimensions as the previous 7/8" LIAD probe, the total sampling areas are equivalent.

Inserted into the hollow outer cylinder is a brass inner cylinder (0.750 in o.d., 0.685 in i.d.) which is held stationary with an aluminum brace. Affixed to the end of the inner cylinder is a specially designed Hydlar coupler and focusing lens cap. Within the coupler, a pair of silver coated reflecting mirrors (Melles-Griot, 5 mm diameter) is mounted onto a removable set of stainless steel plates (0.670 in o.d. \times 0.073 in thick). These two plates and mounted mirrors are referred to as the mirror assembly. The pair of mirrors is designed to reflect the laser beam onto the appropriate desorption axis in alignment with the center of the ICR cell. As previously demonstrated, 10 incomplete overlap between the desorption plume and the stored reagent ions (trapped in the center of the ICR cell) results in decreased ionization efficiency of the desorbed analyte molecules, and hence reduced sensitivity.

Within the mirror assembly, the reflecting mirrors are secured to the plates with a specially designed ball-and-socket mount that facilitates rotational adjustment of the reflecting mirrors. The plates are secured to each other with a set of three stainless steel rods (0.125 in o.d, 0.500 in length). To the end of the set of rods, one of the two plates is secured in three places with a flat-head screw threaded into the end of each rod in order to hold the plate's position stationary. The other plate's position, relative to the first plate, can be adjusted in order to vary the distance between the two mirrors. Adjustment of this distance is accomplished by sliding the second plate along a set of threaded rods (#2–56, 0.112 in diam.) protruding from one end of the stainless steel rods. This three-point mount to which the second of the two plates is secured enables additional adjustment of the angle of this mirror. At the end of the coupler, a Hydlar lens cap containing a focusing lens (Melles-Griot, 5.0 mm diam., 10.0 mm f.l.) is employed to focus the output laser beam onto the backside of the foil in alignment with the magnetic field and appropriate desorption axis.

In the absence of an optical fiber to transmit the laser light down the length of the hollow stainless steel cylinder, a pair of high-energy reflecting mirrors (CVI, 25 mm diam.) are positioned external to the fiberless LIAD probe to direct the laser beam into the probe. The mirrors are secured to a laser table mounted onto the chassis of the instrument. Additionally, a long focal length lens (Melles-Griot, 1000 mm f.l.) is positioned in the beam path to prevent

further divergence of the beam and improve throughput through the mirror assembly. The chassis mounted laser table extends an adequate distance from the probe inlet for easy removal of the laser probe from the instrument without disturbing the external optics. This enables one to easily exchange sample foils and reinsert the fiberless LIAD probe into the instrument without realignment of the laser beam into the outer cylinder.

The fiberless LIAD set-up affords almost an order of magnitude increase in the power density achievable on the backside of the metal foil. With the previous optical fiber containing LIAD probes, achievable power densities were limited to approximately 9.0×10^8 W/cm² due to the damage threshold of the optical fiber (> 4.5 mJ/pulse). Without the use of the power limiting optical fiber, approximately ~50% (12.5 mJ/pulse) of the maximum power (25 mJ/pulse) available from our Nd:YAG laser system can be utilized for acoustic desorption. Reflection losses on the mirrors and lenses, as well as beam divergence over the 2 m (approx.) distance from the laser head to the backside of the foil account for the laser throughput. Power densities of up to 5.0×10^9 W/cm² can be achieved with the new fiberless LIAD probe. This increased power density results in larger amplitude acoustic waves $^{12-14}$ within the sample foil, which increases desorption efficiency. Other than the absence of the optical fiber, the fiberless LIAD probe has a similar general appearance and is operated in a similar manner as the 7/8" conventional LIAD probe.

All compounds were obtained from Sigma Aldrich (St. Louis, MO) except for the tetrapeptide val-ala-ala-phe (Bachem Biosciences, King of Prussia, PA), and the Titanium sample foils (Alfa Aesar, Ward Hill, MA). The compounds and foils were used as received from the supplier. Sample solutions (methanol) were prepared in concentrations ranging from 1 to 10 mM, and they were electrospray deposited ¹⁹ onto Ti metal foils (1.7 cm diam.). By varying the volume of the sprayed solution, sample thicknesses ranging from 30 to 70 nmol/cm² were obtained. The foil was mounted onto the fiberless LIAD probe and inserted into the mass spectrometer to within 1/8" of the source trap plate of the dual cell. The foil was subjected to a series of laser shots (one to two hundred) focused onto the backside of the foil while continually rotating the outer cylinder of the probe. Depending on the input laser power utilized, power densities on the order of 1×10^9 to 5×10^9 W/cm² were obtained on the backside of the foil.

During or following each laser pulse, the analyte molecules were ionized by either electron impact (EI) or chemical ionization (CI). EI of the desorbed neutral molecules was performed by switching the bias of a grid (electron gate) to allow electrons (70 eV electron energy, 5–10 µA emission current, 10–20 ms ionization time) into the ICR cell during or immediately after the laser trigger event (150 μ s duration). Chemical ionization of peptides was achieved by reaction of the desorbed molecules with protonated triethylamine (m/z 102) or diethylaniline (m/z 150) ions stored in the ICR cell. Triethylamine and diethyaniline molecules were introduced through a batch inlet equipped with an Andonian leak valve into one side of the FT-ICR dual cell. The chemical ionization reagent ions were generated through self-chemical ionization processes. ²⁰ This was performed by allowing the molecular ion and its fragment ions, obtained by electron ionization (typically 70 eV electron energy, 5–10 µA emission current, 40 ms ionization time) of the reagent, to react (~2 s) with additional neutral reagent molecules in the cell. The resulting protonated reagent molecules were transferred into the adjacent clean cell through at 2 mm hole in the conductance limit plate by grounding this plate for about 100 μ s. Following transfer, the ions were radiatively ²¹ and collisionally cooled (for approx. 1 s) with a pulse of Ar gas (nominal peak pressure of $\sim 10^{-5}$ torr in the cell). All unwanted ions were ejected from the cell through the use of stored waveform inverse Fourier transform^{22,23} (SWIFT) excitation pulses, leaving the isolated ions of interest in the cell to react with the acoustically desorbed analyte molecules, resulting in ionization.

The flight time distributions of 4-hydroxy- α -cyanocinnamic acid (4HCCA) molecules evaporated from both LIAD probes (fiber and fiberless), were measured utilizing laser irradiances ranging from 9.0×10^8 to 2.5×10^9 W/cm². The method developed here was adapted from a modified gated ion trapping procedure $^{24-26}$ by taking into consideration the evaporation of neutral molecules (as opposed to ions). The mean velocity of the neutral and ionized form of 4HCCA has been previously measured in our laboratories. 4,15 An improved procedure was developed for this work to more accurately take into account the duration of the laser trigger event. In these experiments, the acoustically desorbed molecules (by one laser pulse) were ionized by EI (5 μ s duration, 70 eV, 10 μ A emission current) immediately after a variable flight time (0 to 100 μ s, 5 μ s step size) provided to allow the desorbed molecules to reach the cell after the laser trigger event (150 μ s duration). The percent relative abundance (% RA) of the LIAD evaporated analyte was plotted as a function of flight time for each laser power density used. The data shown are an average of four replicate measurements.

Most of the mass spectra are the result of a single experimental cycle including a set of laser shots (one to two hundred shots), each shot followed by ionization of the desorbed material, and finally simultaneous detection of all ions formed during the total experiment by using a broadband chirp (1.9 kHz to 2.6 MHz, 200 V peak-to-peak, sweep rate 3200 Hz/ μ s) to excite the ions. All data were obtained by collecting 64k data points with an acquisition rate of 8000 kHz. The mass spectra were subjected to baseline correction, Hanning apodization, and one zero-filling.

Results and Discussion

Design and Construction of a High-power LIAD Probe

Implementation of higher laser powers for acoustic desorption in FT-ICR mass spectrometry was accomplished by designing and constructing a new fiberless LIAD probe and the accompanying external optics. A set of mirrors and a focusing lens are used to align the beam from the laser head down the length of the probe. Another set of mirrors is positioned in the tip inside the probe (internal optics) to reflect the beam from the central axis of the probe onto the magnetic field/desorption axis where it is focused onto the backside of the foil.

Alignment of the internal and external optics of the fiberless LIAD setup is required upon installation. Once the optics are appropriately aligned, typically a minimal amount of adjustment of the external optics and no adjustment of the internal optics is required for daily operation of the fiberless LIAD probe. The only instrument modification needed, beyond that required to accommodate the fiber LIAD probes, was the addition of an optical table top (including external alignment mirrors and focusing lens) to the framework of the instrument. Previously, a centering guide ring was installed in the fiber probe insertion path in order to align the desorption axis with the center of the ICR cell. A check of the overall energy throughput of the probe is made prior to use by removing the internal focusing lens and reflecting the laser beam through the conductance limit of the dual cell. An optical window is installed in the beam path (centered with the magnetic field of the instrument) on the opposite end of the FT-ICR to allow transmission and measurement of the probe energy throughput while maintaining high vacuum inside the FT-ICR mass spectrometer. Slight adjustment of the external mirrors can be made to improve the overall energy throughput as needed. Once proper alignment of the beam path through the fiberless LIAD probe is achieved, the fiberless LIAD probe is operated in a similar manner as the conventional fiber containing LIAD probes, with the added feature of the ability to use higher laser powers.

LIAD/CI of higher molecular weight peptides with higher laser powers

The high mass limit for the LIAD/CI analysis of peptides with the fiber LIAD probe is approximately 500 amu. 4,17 This is believed to be due to the limited amplitude of the acoustic wave which can be generated within the sample foil. The use of higher laser irradiances with the "fiberless" LIAD probe enables the high mass limit for biological polymers to be expanded. This is demonstrated, for example, by the successful analysis of the hexapeptide Angiotensin IV (VYIHPF, MW 774). The peptide was electrospray deposited (67 nmol/cm²) onto 12.7 µm thick Ti foil and evaporated utilizing 200 laser shots, each with a power density of $2.3 \times 10^9 \, \text{W/cm}^2$ on the backside of the foil. The peptide molecules were ionized via proton transfer from protonated triethylamine, resulting in generation of the protonated molecule (MH+, m/z 775) and some fragment ions, including the a_4 (m/z 485) and b_4 (m/z 513) ions (Figure 3). The fragmentation is believed to be caused by the high exothermicity of the protonation reaction, and not the desorption event. Similar results were obtained for other peptides that previously could not be detected, including DRVYIHP (MW 899) and QGVYVHPV (MW 899) (data not shown). These results demonstrate that higher laser powers enable the analysis of higher molecular weight peptides.

Assessment of analyte fragmentation with the use of higher laser powers

One of the concerns with utilizing higher laser irradiances for desorption is whether the increased laser energy causes fragmentation of the analyte. It has been established that the laser irradiances used with the fiber LIAD probe (approx. 9×10^8 W/cm²) do not cause analyte fragmentation. ^{9,11} To verify that the same is true for the high-power fiberless LIAD probe, a direct comparison between the results obtained by using the two probes was made. The same sample thickness (83 nmol/cm²) of the tetrapeptide (VAAF) was electrospray deposited onto the Ti foils used in both probes. VAAF was desorbed from both LIAD probes and ionized by proton transfer from protonated diethyaniline (DEAH⁺, m/z 150). Each spectrum (Figure 4) was collected from material desorbed as a result of application of twenty-five laser shots to the backside of the Ti foil while continuously rotating the outer cylinder of the probe to obtain fresh sample desorption areas. Laser pulses with an irradiance of 9.0×10^8 W/cm² (Figure 4a) with the fiber LIAD probe and 2.0×10^9 W/cm² (Figure 4b) and 3.0×10^9 W/cm² (Figure 4c) with the fiberless LIAD probe were utilized. Nearly identical mass spectra were obtained with these different laser powers. Chemical ionization of the desorbed VAAF (proton affinity (PA) = 231.0 kcal/mol²⁸) with protonated diethylaniline (PA = 229.4 kcal/mol²⁹) is expected to result in minimal fragmentation of the peptide due to the low exothermicity of the proton transfer reaction ($\Delta H_{rxn} = -1.6$ kcal/mol). Indeed, only small signals for the major fragment ions 30 y_2 (m/z 237) and b_3 (m/z 242) were detected. The constant product branching ratios for all laser powers demonstrate that the increased laser power does not cause fragmentation of the analyte molecules. This result also confirms that any fragmentation products observed in the mass spectra are due to the exothermicity of the chemical ionization reaction (proton transfer) and not degradation of the analyte molecules upon desorption.

Increased desorption efficiency with higher laser powers

In order to examine the efficiency of desorption at different laser powers, the MALDI matrix 4-hydroxy- α -cyanocinnamic acid (sample thickness approx. 36 nmol/cm²) was desorbed by using single laser pulses with power densities ranging from 1.0×10^9 to 2.5×10^9 W/cm². Digital images of a portion of the sample deposition/desorption side of four fiberless LIAD foils were obtained (Figure 5). Examination of the images revealed that as the power density was increased from 1.0×10^9 W/cm² (Figure 5a) to 1.5×10^9 (Figure 5b), 2.0×10^9 (Figure 5c), and 2.5×10^9 W/cm² (Figure 5d), a significantly greater number of molecules were removed from the surface per laser pulse as evident by the larger spots on the front side of the foil. The desorbed matrix was ionized by electron impact (70 eV), generating the molecular

ion and a minimal amount of fragmentation (data not shown). The general appearance of the spectra obtained was quite similar for the different laser irradiances used. The only observable difference was the increase in the intensity of the molecular ion signal with the use of higher laser powers. This is due to the larger volume of Ti and therefore larger surface area wherein the acoustic wave interacts with the sample. This qualitative comparison demonstrates that increased laser irradiances aide in the evaporation of more material per laser pulse, thus increasing the sensitivity of LIAD analyses.

Assessment of velocity distributions of acoustically desorbed molecules

To further evaluate the influence of the use of higher laser powers with the fiberless LIAD probe, the velocity distributions of LIAD evaporated molecules in an FT-ICR were assessed using several different laser irradiances. The method used here was adapted from a previous procedure $^{4,24-26}$ to take into account the duration of the laser trigger event (150 μ s) and the fact that neutral molecules, as opposed to ions, are desorbed.

The velocity distribution of neutral molecules evaporated by LIAD (fiber or fiberless probes) into an FT-ICR is related to their flight time from the probe tip to the center of the ICR cell. ¹⁵ The flight times were examined by measuring the molecular ion signal intensity, obtained with EI, of a LIAD evaporated analyte after different flight times. The sequence of events is outlined in Figure 6. The experiment consists of a single laser pulse followed by a variable delay (flight time) to allow the desorbed molecules to travel into the cell where they are ionized by EI (5 μ s duration, 70 eV, 10 μ A emission current) and a mass spectrum recorded. Through variation of the flight time from 0 to 85 μ s (5 μ s step size), the velocity distribution of molecules evaporated from the probe is obtained.

With the use of both LIAD probes, laser irradiances of 9.0×10^8 (fiber LIAD probe), 1.0×10^9 , 1.5×10^9 and 2.5×10^9 (fiberless LIAD probe) were used to desorb 4-hydroxy- α -cyanocinnamic acid (4HCCA, MW 189). The ion signal for each flight time and laser power density was obtained from the average of four replicate measurements. The average flight time distributions (Figure 7) show no correlation with the laser irradiance used. This finding demonstrates that the use of higher laser powers with the fiberless LIAD probe does not influence the velocity of the LIAD evaporated molecules.

Conclusions

The high-power laser-induced acoustic desorption probe described here improves the desorption efficiency of higher molecular weight analyte molecules into FT-ICR mass spectrometers because larger amplitude acoustic waves are generated in the Ti sample foil. Further, higher laser irradiances were demonstrated to result in the evaporation of more material per laser pulse from the Ti foil, which results in improved sensitivity. However, higher laser irradiances do not cause fragmentation of the analyte upon desorption nor increase the velocity of the desorbed molecules. Based on the above results and additional evidence presented earlier, ¹⁰ it is concluded to be unlikely that the slower moving thermal wave ¹⁶ plays a role in the acoustic desorption process. Had the desorption process occurred through a thermal mechanism or the desorbed molecules contained excess kinetic energy, additional fragmentation of the peptides studied would have occurred when desorbed with the use of higher laser powers.

Acknowledgements

The authors would like to thank the National Institutes of Health and ExxonMobil Research & Engineering Company for their financial support of this work. The authors also thank Mark Carlsen and Dr. Hartmut Hedderich for their invaluable assistance with instrumentation and helpful discussions.

References

- 1. Lindner B. Int J Mass Spectrom Ion Processes 1991;103:203-218.
- Golovlev VV, Allman SL, Garrett WR, Taranenko NI, Chen CH. Int J Mass Spectrom Ion Processes 1997;169/170:69–78.
- 3. Golovlev VV, Allman SL, Garrett WR, Chen CH. Appl Phys Lett 1997;71:852–854.
- 4. Perez J, Ramirez-Arizmendi LE, Petzold CJ, Guler LP, Nelson ED, Kenttämaa HI. Int J Mass Spectrom 2000;198:173–188.
- Petzold CJ, Ramirez-Arizmendi LE, Heidbrink JL, Perez J, Kenttämaa HI. J Am Soc Mass Spectrom 2002;13:192–194. [PubMed: 11838023]
- 6. Campbell JL, Crawford KE, Kenttämaa HI. Anal Chem 2004;76:959–963. [PubMed: 14961726]
- 7. Campbell JL, Fiddler MN, Crawford KE, Gqamana PP, Kenttämaa HI. Anal Chem 2005;77:4020–4026. [PubMed: 15987106]
- 8. Crawford KE, Campbell JL, Fiddler MN, Duan P, Qian K, Gorbaty ML, Kenttämaa HI. Anal Chem 2005;77:7916–7923. [PubMed: 16351138]
- 9. Liu J, Petzold CJ, Ramirez-Arizmendi LE, Perez J, Kenttämaa H. J Am Chem Soc 2005;127:12758–12759. [PubMed: 16159243]
- 10. Shea RC, Campbell JL, Petzold CJ, Li S, Aaserud DJ, Kenttämaa HI. Anal Chem. 2006In Press
- 11. Shea, R. C.; Petzold, C. J.; Liu, J.; Li, S.; Kenttämaa, H. I. unpublished work.
- 12. Anderholm NC. Appl Phys Lett 1970;16:113-115.
- 13. Yang LC. J Appl Phys 1974;45:2601-2608.
- 14. Yaakobi B, Boehly T, Bourke P, Conturie Y, Craxton RS, Delettrez J, Forsyth JM, Frankel RD, Goldman LM, et al. Opt Commun 1981;39:175–179.
- Perez J, Petzold CJ, Watkins MA, Vaughn WE, Kenttämaa HI. J Am Soc Mass Spectrom 1999;10:1105–1110. [PubMed: 10536817]
- Scruby, CB.; Drain, LE. Laser Ultrasonics: Techniques and Applications. Adam Hilger; New York: 1990.
- 17. Petzold, CJ. Ph.D Thesis. Purdue University; West Lafayette, IN: 2002.
- 18. Leeck DT, Stirk KM, Zeller LC, Kiminkinen LKM, Castro LM, Vainiotalo P, Kenttämaa HI. J Am Chem Soc 1994;116:3028–3038.
- 19. NcNeal CJ, Macfarlane RD, Thurston EL. Anal Chem 1979;51:2036-2039.
- 20. Ghaderi S, Kulkarni PS, Ledford EB, Wilkins CL, Gross ML. Anal Chem 1981;53:428-437.
- 21. Dunbar RC. Mass Spectrom Rev 1992;11:309-339.
- 22. Marshall AG, Wang TCL, Ricca TL. J Am Chem Soc 1985;107:7893–7897.
- 23. Chen L, Wang TC, Ricca TL, Marshall AG. Anal Chem 1987;59:449-454. [PubMed: 3565762]
- 24. Castoro JA, Koster C, Wilkins CL. Rapid Commun in Mass Spectrom 1992;6:239-241.
- 25. Koster C, Castoro JA, Wilkins CL. J Am Chem Soc 1992;114:7572–7574.
- 26. Yao J, Dey M, Pastor SJ, Wilkins CL. Anal Chem 1995;67:3638–3642. [PubMed: 8644917]
- 27. Immediately following application of the laser trigger event, a Q-switch delay of approximately 150 μ s is followed by a 60 ns build-up time and emission of the 3 ns wide laser pulse from the flashlamp of the laser; Part Number 996–0220, R. B., Ed.: Continuum Lasers, Santa Clara, CA, 1997.
- 28. The proton affinity of VAAF was bracketed to 231.0 kcal/mol by examining the reactivity of the LIAD desorbed peptide with a proton transfer reagent that did and did not result in ionization of the peptide. VAAF was observed to abstract a proton from protonated diethylaniline (PA =229.4 kcal/mol²⁹) but not from protonated triphenylphosphine (PA = 232.5 kcal/mol²⁹).
- 29. Hunter, EP.; Lias, SG. NIST Standard Reference Database. National Institute of Standards and Technology; Gaithersburg, MD: 2001.
- 30. Biemann K. Acc Chem Res 1994;24:370-378.
- 31. The flight time distribution of LIAD-evaporated molecules is estimated to be approximately 30 to 50 μ s. A low intensity (< 10% relative abundance) "tail" extends out to approximately 1000 μ s.

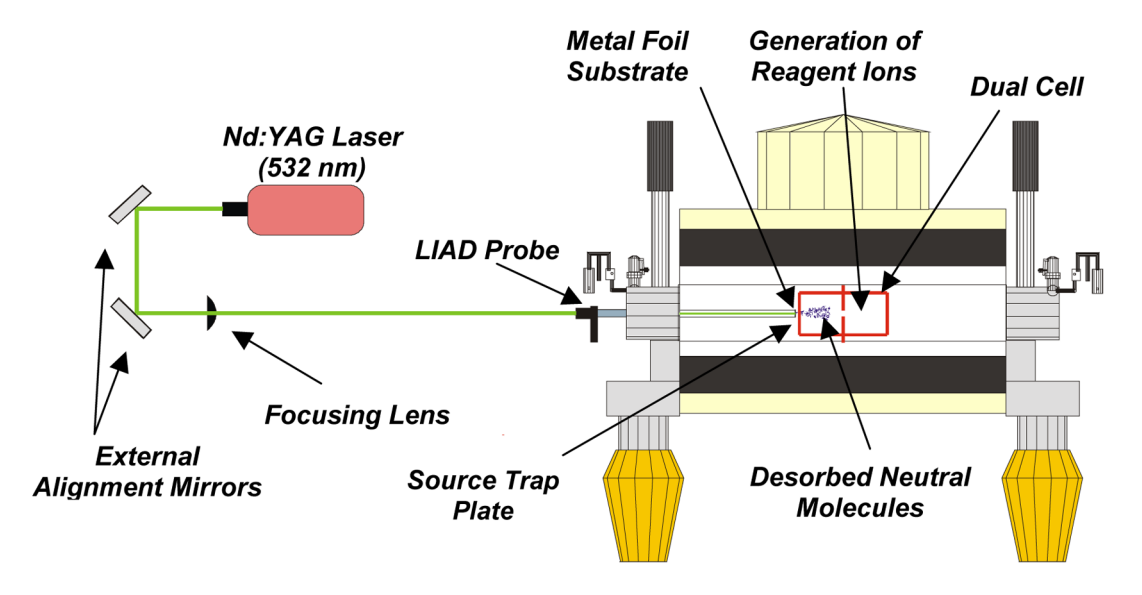


Figure 1. Diagram of the fiberless LIAD setup for a dual cell FT-ICR mass spectrometer.

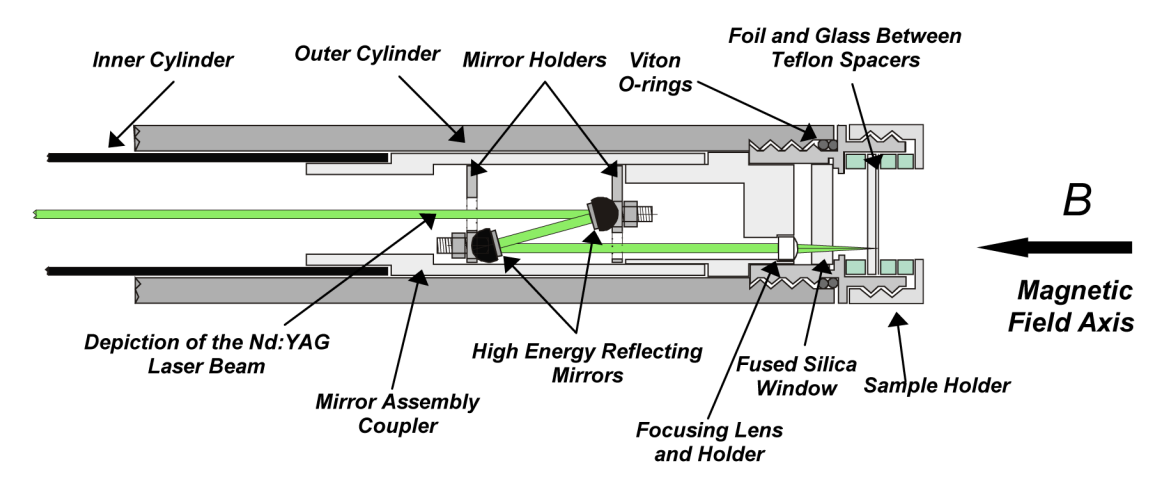


Figure 2. Diagram of the laser beam reflection and focusing region of the fiberless LIAD probe.

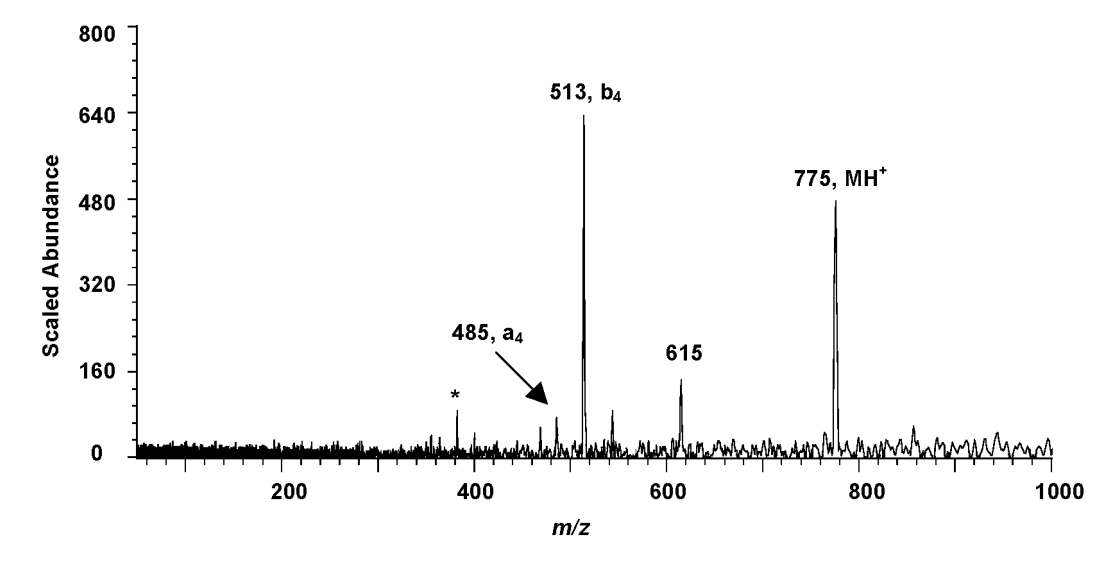


Figure 3. A LIAD/CI mass spectrum of Angiotensin IV (VYIHPF, MW 774) evaporated by using a power density of 2.3×10^9 W/cm² in the fiberless LIAD probe (200 laser shots) and ionized by proton transfer from protonated triethylamine (m/z 102). * Background.

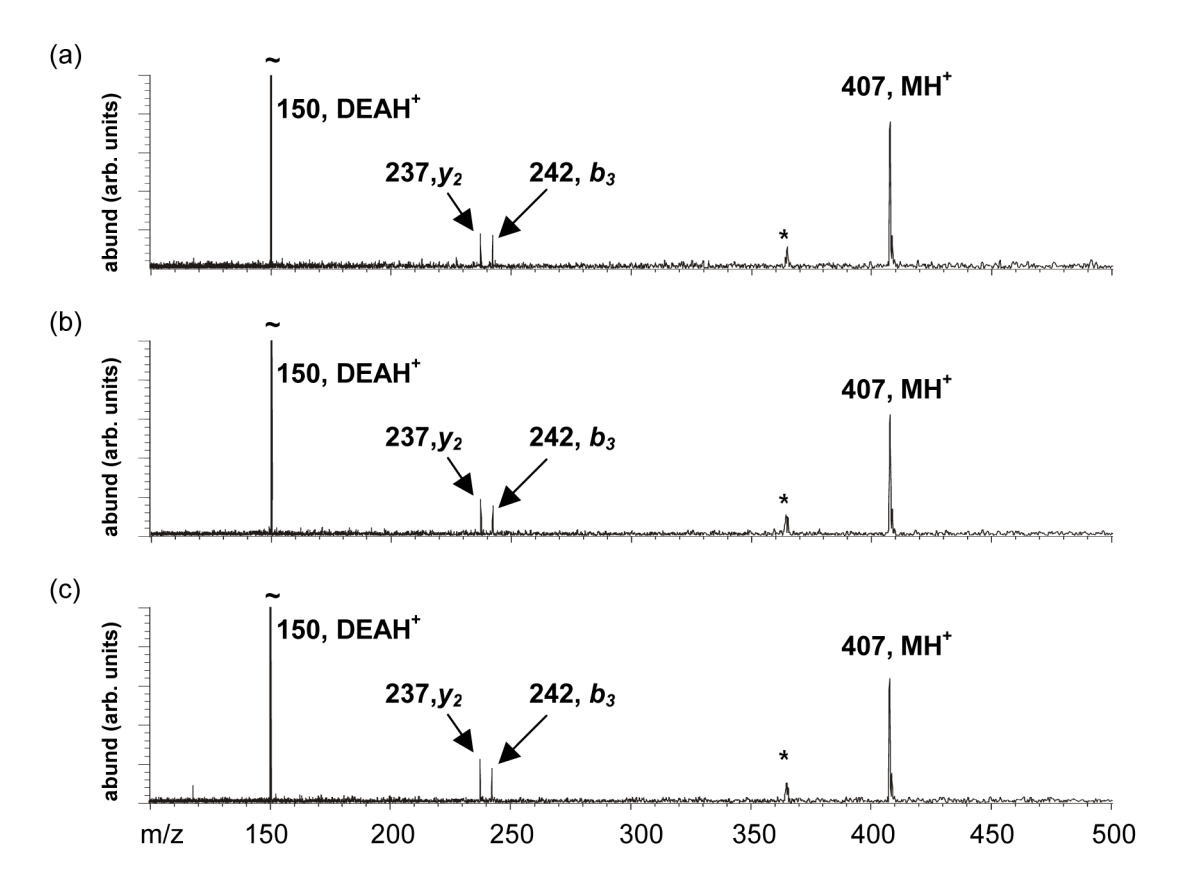


Figure 4. LIAD/CI mass spectra (25 laser shots per spectrum) of VAAF obtained by using (a) the conventional (optical fiber) LIAD probe at a power density of 9.0×10^8 W/cm², (b) the fiberless LIAD probe at a power density of 2.0×10^9 W/cm² and (c) a power density of 3.0×10^9 W/cm² (on the backside of the foil) and proton transfer from protonated diethylaniline (DEAH⁺, m/z 150) to ionize VAAF. * Background.

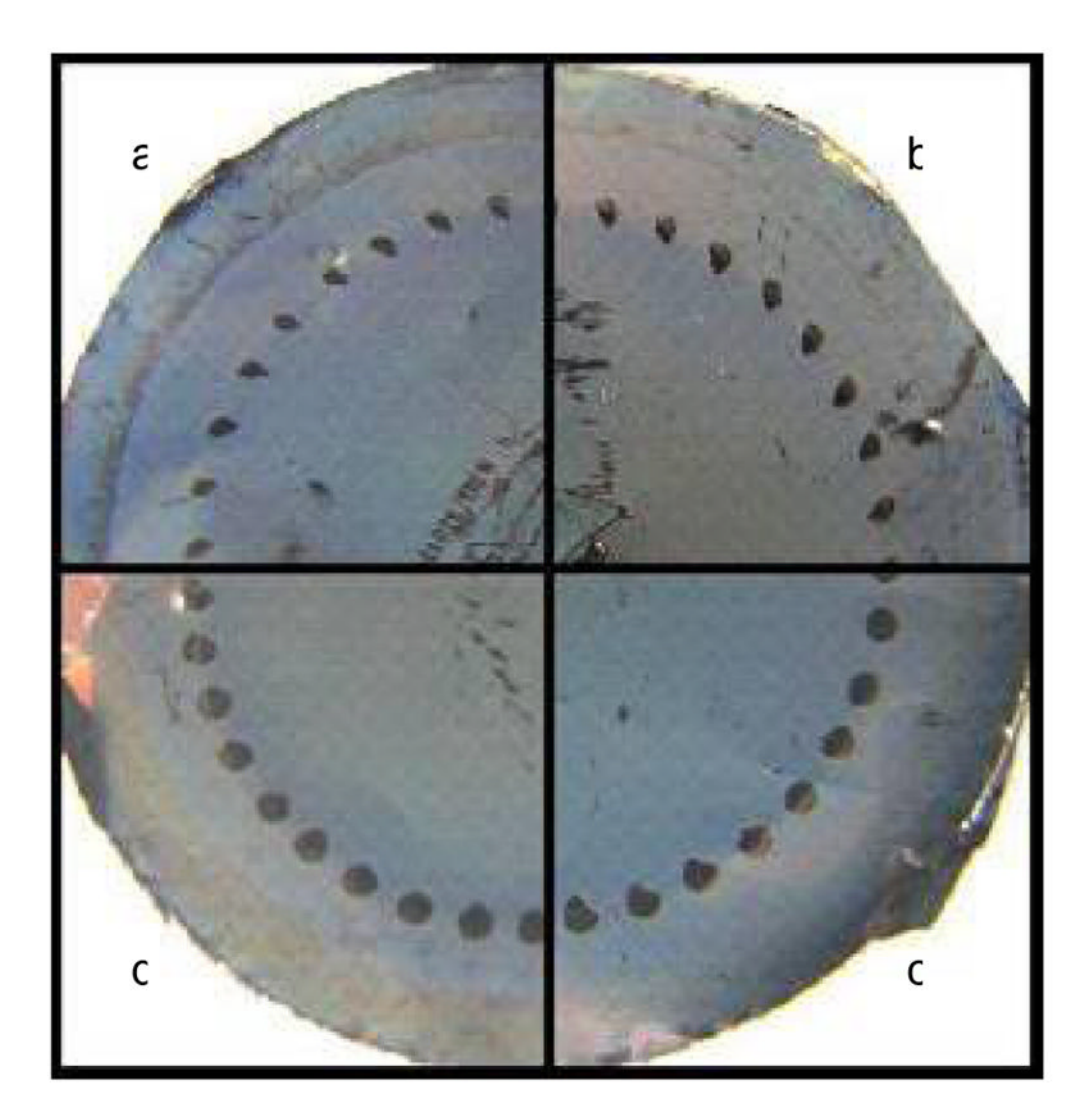


Figure 5. Digital images of a portion of the sample side of four fiberless LIAD foils after desorption. The individual foils were electrospray coated with the MALDI matrix 4-hydroxy-α-cyanocinnamic acid which was desorbed into a FT-ICR mass spectrometer with single laser shots of power densities of (a) 1.0×10^9 , (b) 1.5×10^9 , (c) 2.0×10^9 and (d) 2.5×10^9 W/cm². Subjection of the foil to higher laser powers results in evaporation of more molecules per laser shot as indicated by the larger areas from which the sample has been removed from the foil surface.

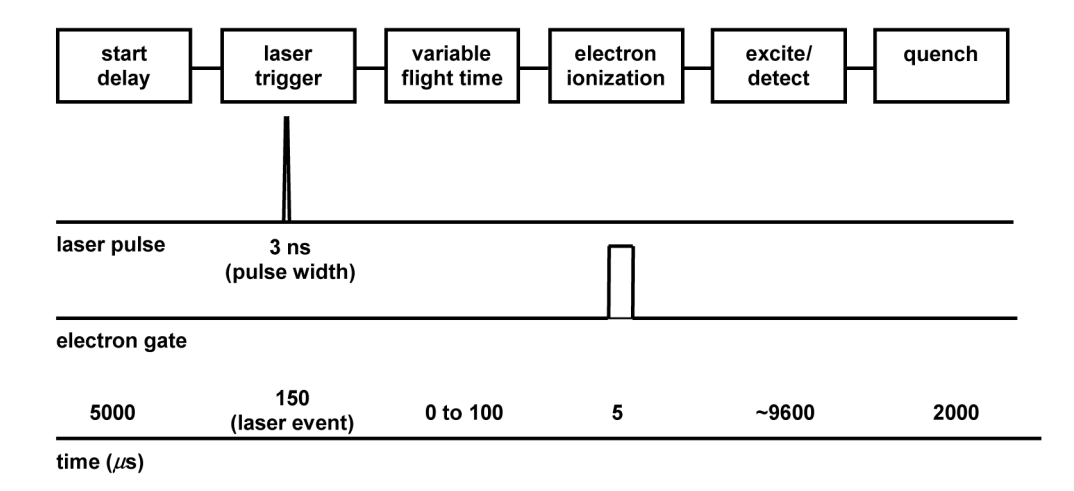


Figure 6.

Event sequence used for assessment of the flight time distribution of LIAD evaporated molecules from the fiber and fiberless LIAD probes. The relative abundance of the desorbed molecules, ionized by electron impact (70 eV, $10 \mu A$, $5 \mu s$ duration), was measured as a function of the variable flight time (0 to $85 \mu s$) after application of the laser trigger (150 μs laser event containing a 3 ns long laser pulse).

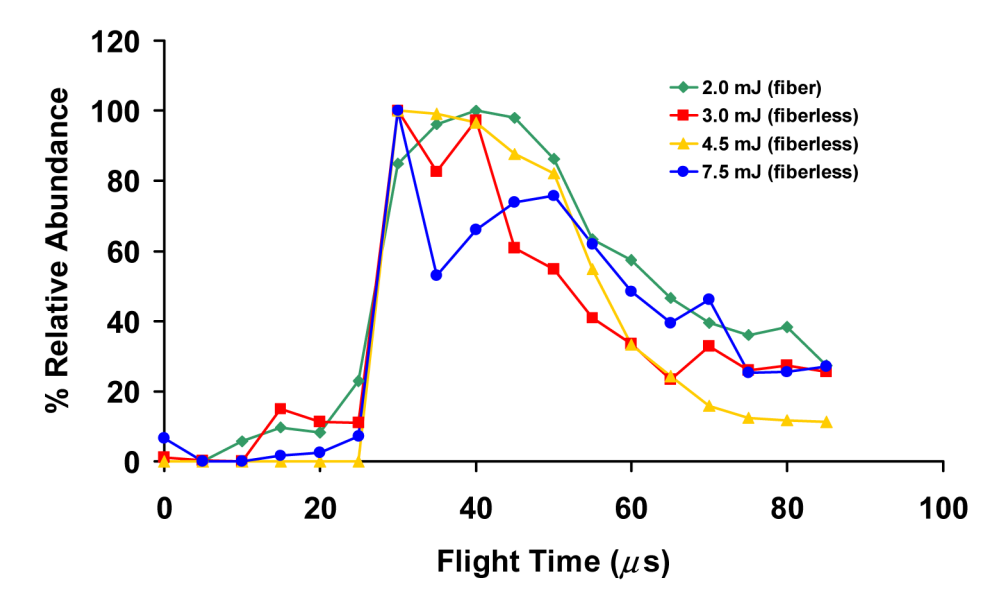


Figure 7. Average (of four measurements) distributions of flight time of 4-hydroxy- α -cyanocinnamic acid (4HCCA, m/z 189) from the sample foil to near the center of the ICR cell. Ions were generated by electron ionization (70 eV, 10 μ A, 5 μ s duration) of the LIAD evaporated molecules (LIAD/EI) after a variable flight time (0 to 85 μ s) following application of the laser trigger (0.150 μ s). The average flight time distributions of molecules evaporated by LIAD from the fiber probe (2.0 mJ/pulse on the backside of the foil) and fiberless LIAD probe (3.0, 4.5 and 7.5 mJ/pulse on the backside of the foil) are similar.